

Supporting Information for:

# Synthesis and Self-Aggregated Nanostructures of Hydrogen-Bonding Polydimethylsiloxane

Senbin Chen,<sup>\*a</sup> Yanggui Wu,<sup>a</sup> Huiying Wang,<sup>a</sup> Bengao Zhu,<sup>a</sup> Bijing Xiong,<sup>a</sup> Wolfgang H.  
Binder<sup>\*b</sup> and Jintao Zhu<sup>\*a</sup>

<sup>a</sup>: Key Laboratory of Materials Chemistry for Energy Conversion and Storage of Ministry of Education, School of Chemistry and Chemical Engineering, Huazhong University of Science and Technology, Wuhan 430074, China

<sup>b</sup>: Chair of Macromolecular Chemistry, Faculty of Natural Science II (Chemistry, Physics and Mathematics), Martin Luther University Halle-Wittenberg, von-Danckelmann-Platz 4, Halle (Saale) D-06120, Germany

Correspondence to: J. Zhu (jtzhu@mail.hust.edu.cn)

W. H. Binder (wolfgang.binder@chemie.uni-halle.de)

S. Chen (senbin@hust.edu.cn)

## Table of Contents:

Experimental section.....	3
Materials .....	3
Characterization methods.....	3
Synthesis of TAP-PDMS (Figure S1).....	5
Synthesis of Ba-PDMS (Figure S3) .....	9
MALDI-TOF MS measurement of Ba-PDMS1 and Ba-PDMS3 .....	12
MALDI-TOF MS measurement of HW-PDMS1 and HW-PDMS3 .....	15
<sup>1</sup> H NMR spin-lattice relaxation time T1 calculation.....	18
SAXS profile of HO-PDMS1.....	18
Mathematical model chosen to determine K <sub>a</sub> between Ba-PDMS1 and TAP-PDMS1. ....	18
Mathematical model chosen to determine K <sub>a</sub> between Ba-PDMS1 and HW-PDMS1. ....	20
Viscosities of H-bonding PDMS.....	21
SAXS profiles of H-bonding PDMS.....	22
References.....	22

## Experimental section

### Materials

$\alpha$ -Mono-carbinol functionalized PDMS (OH-PDMS1, 2 and 3) were purchased from Gelest, Inc. All the other chemicals were purchased from Alfa Aesar or Sigma-Aldrich. Unless otherwise indicated the other chemicals were used without further purification. HW-PDMS1,<sup>1</sup> 2<sup>2</sup> and 3<sup>1</sup> were synthesized according to previous works.

### Characterization methods

<sup>1</sup>H, <sup>13</sup>C and <sup>29</sup>Si NMR spectra were recorded on Varian Gemini 2000 FT-NMR spectrometer (400 MHz) or Varian unity Inova 500 (500 MHz) NMR spectrometer, using CDCl<sub>3</sub> or DMSO-d<sub>6</sub> as solvent. The <sup>1</sup>H T1 relaxation was determined using the inversion recovery method.

Polymers were analyzed by size exclusion chromatography (SEC) running in THF at 35°C (flow rate: 1 mL·min<sup>-1</sup>) and recorded on GPCmax VE 2001 from Viscotek™, which equipped with a column set of a H<sub>HR</sub>-H Guard-17369 column, a CLM30111 column and a G2500H<sub>HR</sub>-17354 column. The average molar mass of polymers was derived from refractive index signal based on polystyrene calibration curve.

Matrix-assisted laser desorption/ionization time of flight mass spectrometry (MALDI-TOF MS) measurements were performed on Bruker Autoflex III system (Bruker Daltonics) operating in linear mode. Data evaluation was carried out on DataAnalysis software. Ions were formed by laser desorption (smart beam laser at 355, 532, 808, and 1064 ± 5 nm; up to 50 Hz repetition rate), accelerated by a voltage of 20 kV and detected as positive ions. Samples were

prepared by mixing 50  $\mu\text{L}$  of 2,5-dihydroxybenzoic acid at 20  $\text{g}\cdot\text{L}^{-1}$  in THF with 10  $\mu\text{L}$  of polymer solution at 20  $\text{g}\cdot\text{L}^{-1}$  in THF. To enhance cationization of polymers, 1  $\mu\text{L}$  of NaI at 10  $\text{g}\cdot\text{L}^{-1}$  in acetone was added to solutions. Finally, 1  $\mu\text{L}$  of resulting mixture was spotted on a MALDI sample plate and air-dried.

The solid-state NMR measurements were carried out at a  $^1\text{H}$  Larmor frequency of 400 MHz on a Bruker Avance III spectrometer with double- or triple-resonance 4 mm MAS probes. The samples were packed into 4 mm  $\text{ZrO}_2$  rotors using Kel-F inserts and Vespel caps and spun at 10 kHz. The temperature regulation was based upon heated pressurized air using a BVT3000 temperature control unit, with an accuracy of around 1K. Fully relaxed  $^1\text{H}$  spectra (recycle delay of  $5T_1$ ) were taken after a  $90^\circ$  pulse of 3.12  $\mu\text{s}$  duration. To obtain qualitative information on mobility,  $T_2$  relaxation times were measured using a rotor-synchronized Hahn-echo pulse sequence.

Small angle X-ray scattering (SAXS) experiments were performed with the rotating anode from Rigaku company. The wavelength of X-ray (Cu  $K\alpha$ ) is  $\lambda = 1.54 \text{ \AA}$ . The tube voltage and tube current were 40 kv and 60 mA. Through the optics and three pinholes, the X-ray beam become collimated and small sized. The sample holder was an aluminum disc with a hole of diameter of 1 mm in the middle. The sample was placed into the hole, and the aluminum disc was attached onto a Linkam hot stage TMS 94 by thermal conducting paste. Temperature-dependent SAXS measurements were done for all the samples at a broad temperature range, from 20 to maximum 180  $^\circ\text{C}$ . The measured  $q$  range was from 0.04 to 0.4  $\text{\AA}^{-1}$ .

## **Synthesis of TAP-PDMS (Figure S1)**

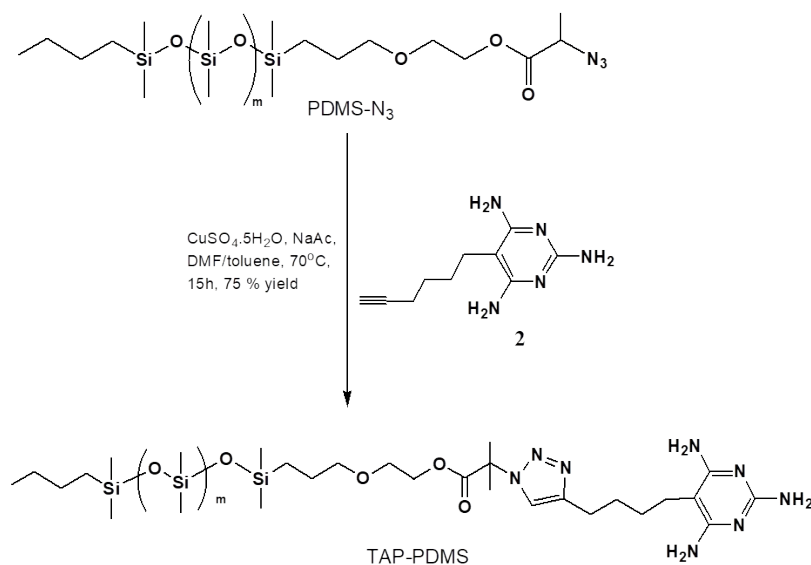


**Figure S1:** Synthetic route to TAP-PDMS.

In this context, a general procedure for the synthesis of TAP-PDMS1, 2 and 3 (**Figure S1**) was shown via the PDMS-N<sub>3</sub> with Mn = 11.4 kDa. PDMS-N<sub>3</sub> (Mn = 11.4 kDa, 0.15 g, 0.013 mmol) was dissolved in 2 mL toluene, compound **2**<sup>2</sup> (0.0025 g, 0.013 mmol) was fully dissolved in 0.75 mL DMF, then the two obtained solutions were mixed together in a round-bottomed flask. Sodium L-ascorbate (0.013 g, 0.065 mmol) was added, and the mixture was degassed by bubbling N<sub>2</sub> for ~30 min. CuSO<sub>4</sub>·5H<sub>2</sub>O (0.0032 g, 0.013 mmol) was added to the mixture which was degassed again by bubbling N<sub>2</sub> for ~30 min, and then allowed to stir at 70 °C for 15 h. The mixture was cooled, concentrated, dissolved in CH<sub>2</sub>Cl<sub>2</sub>, and filtered to remove CuSO<sub>4</sub>·5H<sub>2</sub>O and sodium L-ascorbate, and then the filtrate was purified by column chromatography (eluent: CH<sub>2</sub>Cl<sub>2</sub>/MeOH, 100/3, v/v) to give TAP-PDMS3 as a yellowish viscous solid (0.13g, yield 75%).

<sup>1</sup>H NMR (CDCl<sub>3</sub>, **Figure S2A**) δ (ppm): 0.07 (s, ~84H), 0.52 (m, 4H), 0.88 (t, 3H), 1.31 (m, 4H), 1.48 (br, 2H), 1.59 (sext, 2H), 1.85 (m, 2H), 2.44 (br, 2H), 2.86 (br, 2H), 3.42 (t, 2H),

3.64 (t, 2H), 4.31 (m, 2H), 5.46 (br, 2H), 5.75 (br, 2H), 6.13 (br, 4H), 7.54 (br, 1H).

$^{13}\text{C}$  NMR ( $\text{CDCl}_3$ , **Figure S2B**)  $\delta$  (ppm): 0.88, 1.02, 10.81, 13.76, 14.07, 17.86, 23.33, 25.41, 26.32, 28.91, 29.69, 30.35, 38.88, 65.32, 68.00, 71.70, 74.07, 86.01, 128.80, 130.94, 132.54, 152.61, 167.97, 169.52.

$^{29}\text{Si}$  NMR ( $\text{CDCl}_3$ , **Figure S2C**)  $\delta$  (ppm): -22.28.

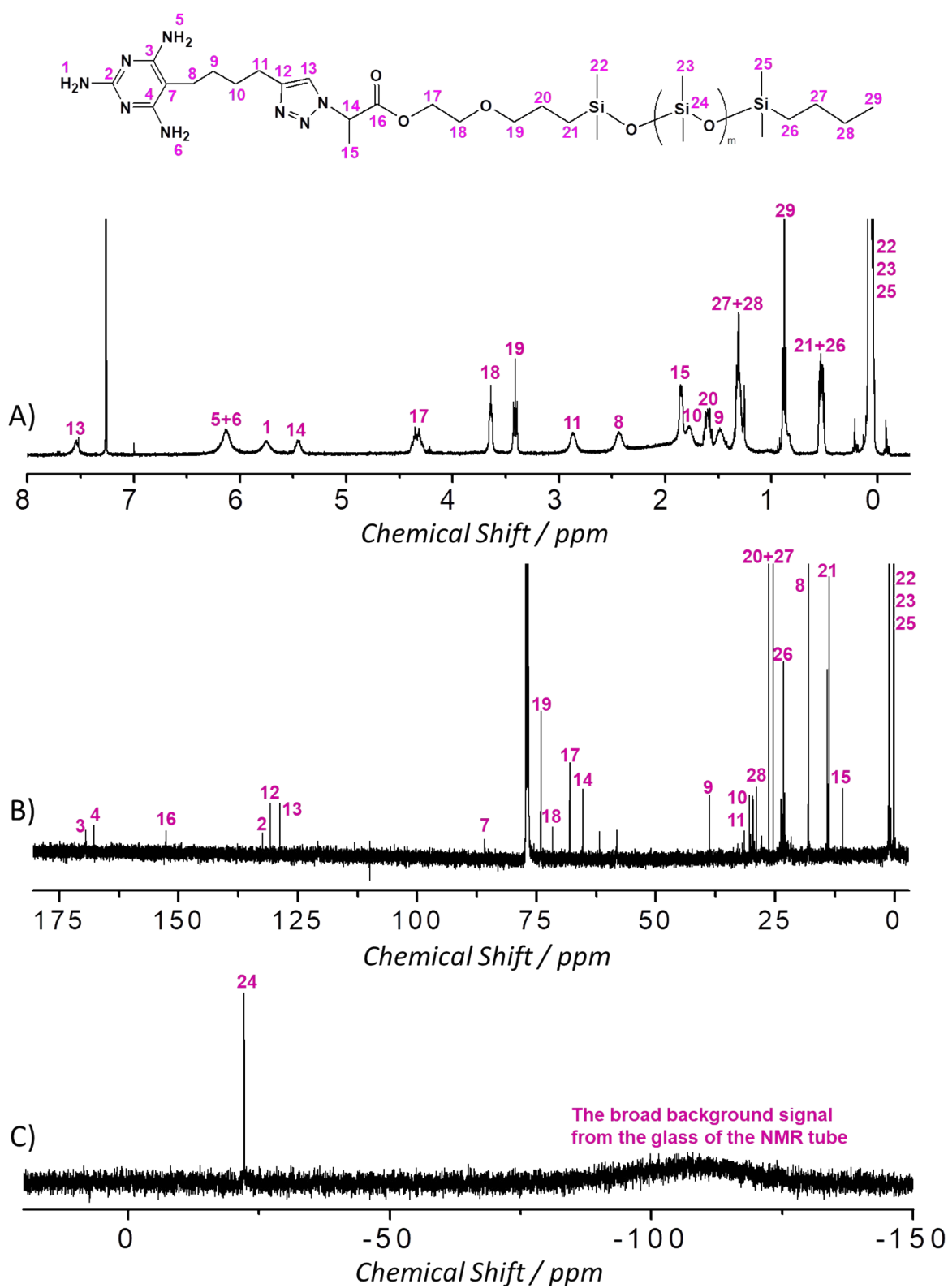


**Figure S2:**  $^1\text{H}$  (A),  $^{13}\text{C}$  (B) and  $^{29}\text{Si}$  (C) of TAP-PDMS1 recorded in  $\text{CDCl}_3$  at 27 °C.

**Table S1:** MALDI-TOF MS results of TAP-PDMS1.

Series	Species	m/z <sub>measured</sub>	m/z <sub>simulated</sub>
		g·mol <sup>-1</sup>	g·mol <sup>-1</sup>
①	[C <sub>18</sub> H <sub>29</sub> N <sub>8</sub> O <sub>3</sub> (C <sub>2</sub> H <sub>6</sub> OSi) <sub>7</sub> C <sub>6</sub> H <sub>15</sub> Si + H] <sup>+</sup>	1039.482	1039.469
②	[C <sub>18</sub> H <sub>29</sub> N <sub>8</sub> O <sub>3</sub> (C <sub>2</sub> H <sub>6</sub> OSi) <sub>7</sub> C <sub>6</sub> H <sub>15</sub> Si + Li <sub>2</sub> - H] <sup>+</sup>	1051.534	1051.486
③	[C <sub>18</sub> H <sub>29</sub> N <sub>8</sub> O <sub>3</sub> (C <sub>2</sub> H <sub>6</sub> OSi) <sub>7</sub> C <sub>6</sub> H <sub>15</sub> Si + Na] <sup>+</sup>	1061.509	1061.451
④	[C <sub>18</sub> H <sub>29</sub> N <sub>8</sub> O <sub>3</sub> (C <sub>2</sub> H <sub>6</sub> OSi) <sub>8</sub> C <sub>6</sub> H <sub>15</sub> Si + H] <sup>+</sup>	1113.533	1113.488
⑤	[C <sub>18</sub> H <sub>29</sub> N <sub>8</sub> O <sub>3</sub> (C <sub>2</sub> H <sub>6</sub> OSi) <sub>8</sub> C <sub>6</sub> H <sub>15</sub> Si + Li] <sup>+</sup>	1119.429	1119.496
⑥	[C <sub>18</sub> H <sub>29</sub> N <sub>8</sub> O <sub>3</sub> (C <sub>2</sub> H <sub>6</sub> OSi) <sub>9</sub> C <sub>6</sub> H <sub>15</sub> Si + H] <sup>+</sup>	1188.106	1188.507
⑦	[C <sub>18</sub> H <sub>29</sub> N <sub>8</sub> O <sub>3</sub> (C <sub>2</sub> H <sub>6</sub> OSi) <sub>9</sub> C <sub>6</sub> H <sub>15</sub> Si + Li] <sup>+</sup>	1193.526	1193.515
⑧	[C <sub>18</sub> H <sub>29</sub> N <sub>8</sub> O <sub>3</sub> (C <sub>2</sub> H <sub>6</sub> OSi) <sub>10</sub> C <sub>6</sub> H <sub>15</sub> Si + H] <sup>+</sup>	1262.557	1262.526

**Table S2:** MALDI-TOF MS results of TAP-PDMS2.

Series	Species	m/z <sub>measured</sub>	m/z <sub>simulated</sub>
		g·mol <sup>-1</sup>	g·mol <sup>-1</sup>
①	[C <sub>18</sub> H <sub>29</sub> N <sub>8</sub> O <sub>3</sub> (C <sub>2</sub> H <sub>6</sub> OSi) <sub>67</sub> C <sub>6</sub> H <sub>15</sub> Si + H] <sup>+</sup>	5489.503	5489.596
②	[C <sub>18</sub> H <sub>29</sub> N <sub>8</sub> O <sub>3</sub> (C <sub>2</sub> H <sub>6</sub> OSi) <sub>67</sub> C <sub>6</sub> H <sub>15</sub> Si + Na] <sup>+</sup>	5511.497	5511.578
③	[C <sub>18</sub> H <sub>29</sub> N <sub>8</sub> O <sub>3</sub> (C <sub>2</sub> H <sub>6</sub> OSi) <sub>68</sub> C <sub>6</sub> H <sub>15</sub> Si + H] <sup>+</sup>	5563.536	5563.615
④	[C <sub>18</sub> H <sub>29</sub> N <sub>8</sub> O <sub>3</sub> (C <sub>2</sub> H <sub>6</sub> OSi) <sub>68</sub> C <sub>6</sub> H <sub>15</sub> Si + Na] <sup>+</sup>	5585.508	5585.597
⑤	[C <sub>18</sub> H <sub>29</sub> N <sub>8</sub> O <sub>3</sub> (C <sub>2</sub> H <sub>6</sub> OSi) <sub>69</sub> C <sub>6</sub> H <sub>15</sub> Si + Na] <sup>+</sup>	5659.531	5659.615
⑥	[C <sub>18</sub> H <sub>29</sub> N <sub>8</sub> O <sub>3</sub> (C <sub>2</sub> H <sub>6</sub> OSi) <sub>70</sub> C <sub>6</sub> H <sub>15</sub> Si + H] <sup>+</sup>	5711.574	5711.652
⑦	[C <sub>18</sub> H <sub>29</sub> N <sub>8</sub> O <sub>3</sub> (C <sub>2</sub> H <sub>6</sub> OSi) <sub>70</sub> C <sub>6</sub> H <sub>15</sub> Si + Na] <sup>+</sup>	5733.566	5733.634

**Table S3:** MALDI-TOF MS results of TAP-PDMS3.

Series	Species	m/z <sub>measured</sub>	m/z <sub>simulated</sub>
		g·mol <sup>-1</sup>	g·mol <sup>-1</sup>
①	[C <sub>18</sub> H <sub>29</sub> N <sub>8</sub> O <sub>3</sub> (C <sub>2</sub> H <sub>6</sub> OSi) <sub>118</sub> C <sub>6</sub> H <sub>15</sub> Si + H] <sup>+</sup>	9271.486	9271.553
②	[C <sub>18</sub> H <sub>29</sub> N <sub>8</sub> O <sub>3</sub> (C <sub>2</sub> H <sub>6</sub> OSi) <sub>118</sub> C <sub>6</sub> H <sub>15</sub> Si + Na] <sup>+</sup>	9293.462	9293.535
③	[C <sub>18</sub> H <sub>29</sub> N <sub>8</sub> O <sub>3</sub> (C <sub>2</sub> H <sub>6</sub> OSi) <sub>119</sub> C <sub>6</sub> H <sub>15</sub> Si + H] <sup>+</sup>	9345.503	9345.571
④	[C <sub>18</sub> H <sub>29</sub> N <sub>8</sub> O <sub>3</sub> (C <sub>2</sub> H <sub>6</sub> OSi) <sub>119</sub> C <sub>6</sub> H <sub>15</sub> Si + Na] <sup>+</sup>	9367.479	9367.553
⑤	[C <sub>18</sub> H <sub>29</sub> N <sub>8</sub> O <sub>3</sub> (C <sub>2</sub> H <sub>6</sub> OSi) <sub>120</sub> C <sub>6</sub> H <sub>15</sub> Si + Na] <sup>+</sup>	9441.508	9441.572
⑥	[C <sub>18</sub> H <sub>29</sub> N <sub>8</sub> O <sub>3</sub> (C <sub>2</sub> H <sub>6</sub> OSi) <sub>121</sub> C <sub>6</sub> H <sub>15</sub> Si + H] <sup>+</sup>	9493.517	9493.609
⑦	[C <sub>18</sub> H <sub>29</sub> N <sub>8</sub> O <sub>3</sub> (C <sub>2</sub> H <sub>6</sub> OSi) <sub>121</sub> C <sub>6</sub> H <sub>15</sub> Si + Na] <sup>+</sup>	9515.536	9515.591

## Synthesis of Ba-PDMS (Figure S3)

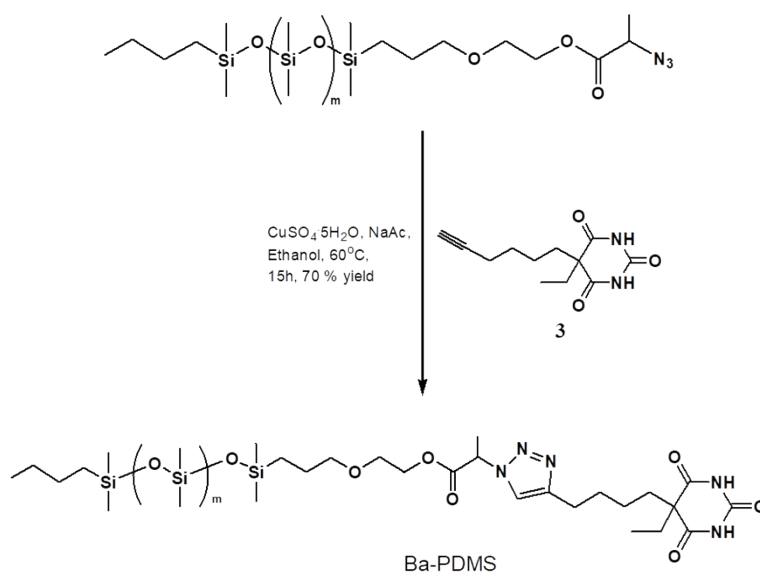


**Figure S3:** Synthetic route to Ba-PDMS.

In this context, a general procedure for the synthesis of Ba-PDMS1, 2 and 3 (**Figure S3**) was

shown via the PDMS- N<sub>3</sub> with Mn = 11.4 kDa. PDMS-N<sub>3</sub> (0.33 g, 0.26 mmol) and compound **3** (0.91 g, 0.4 mmol) were added to a round-bottomed flask and dissolved in ethanol (5 mL). Sodium L-ascorbate (0.021 g, 0.1 mmol) was added, and the mixture was degassed by bubbling N<sub>2</sub> for ~30 min. CuSO<sub>4</sub>·5H<sub>2</sub>O (0.0064 g, 0.026 mmol) was added, the flask was degassed again by bubbling N<sub>2</sub> for ~30 min, and then allowed to stir at 60 °C for 15 h. The mixture was cooled, concentrated, dissolved in CH<sub>2</sub>Cl<sub>2</sub>, and filtered to remove CuSO<sub>4</sub>·5H<sub>2</sub>O and sodium L-ascorbate, and then the filtrate was purified by column chromatography (eluent: CH<sub>2</sub>Cl<sub>2</sub>/MeOH, 100/3, v/v) to give Ba-PDMS as a yellowish solid (yield 70%).

<sup>1</sup>H NMR (CDCl<sub>3</sub>, **Figure S4A**) δ (ppm): 0.07 (s, ~84H), 0.54 (m, 4H), 0.88 (t, 3H), 0.92 (t, 3H), 1.25-1.31 (m, 6H), 1.56-1.68 (m, 4H), 1.82 (d, 3H), 2.03 (m, 4H), 2.74 (br, 3H), 3.45 (t, 2H), 3.67 (t, 2H), 4.34 (m, 2H), 5.46 (q, 1H), 7.43 (s, 1H), 8.56 (br.s, 2H).

<sup>13</sup>C NMR (CDCl<sub>3</sub>, **Figure S4B**) δ (ppm): 0.94, 9.14, 13.75, 13.77, 17.80, 22.99, 25.32, 26.00, 30.99, 32.27, 33.61, 57.02, 57.99, 64.93, 67.90, 73.87, 121.01, 142.18, 147.78, 168.89, 172.16.

<sup>29</sup>Si NMR (CDCl<sub>3</sub>, **Figure S4C**) δ (ppm): -22.38.

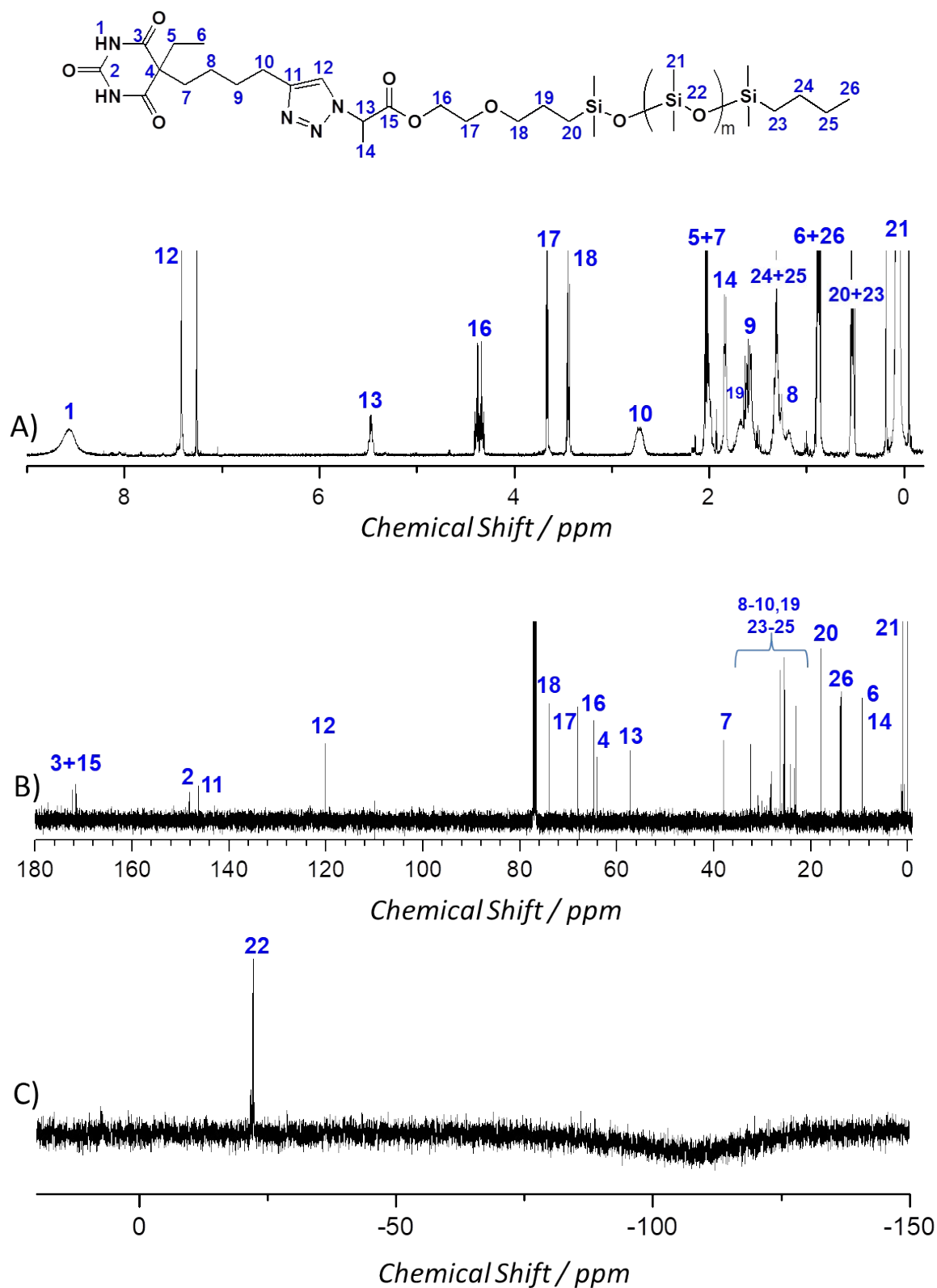


**Figure S4:** <sup>1</sup>H (A), <sup>13</sup>C (B) and <sup>29</sup>Si (C) of Ba-PDMS1 recorded in CDCl<sub>3</sub> at 27 °C.

## MALDI-TOF MS measurement of Ba-PDMS1 and Ba-PDMS3

The structure of Ba-PDMS was further studied via MALDI-TOF MS spectrometry (**Figure S5**).

The mass spectrum of Ba-PDMS1 was observed in the linear mode, **Figure S5A** was obtained by ionization of chains assisted with 2,5-dihydroxybenzoic acid as matrix and NaI as cationization agent. MALDI-TOF spectrum (**Figure S5B**) underlined the presence of main series (① and ⑬), along with other minor series (②-⑫), the mass difference between the  $m/z$  values of molecular ions between series ①, ⑥, ⑩ and ⑬ was equal to  $\sim 74.0$  g/mol, reflecting the repeating dimethylsiloxane units (calculated 74.02 g/mol). The observation of the main series (①) visible at 1552.533 g/mol (**Figure S5C**) could be assigned to a Ba functionalized species  $[\text{C}_6\text{H}_{15}\text{Si-P(DMS)}_{13}\text{-Ba} + \text{Na}]^+$ , i.e.,  $[\text{C}_6\text{H}_{15}\text{Si-P(C}_2\text{H}_6\text{OSi)}_{13}\text{-C}_{21}\text{H}_{34}\text{N}_5\text{O}_6 + \text{Na}]^+$ , which matched well with simulated pattern ( $m/z_{\text{average}} = 1552.579$  g/mol). The observed isotopic patterns of other minor series (②-⑬), illustrated in **Figure S5B**, also agreed well with the simulated structures, illustrating the click reaction proceeded effectively, and ascertaining the successful formation of barbiturate functionalized PDMS (Ba-PDMS1). Additionally, the structure of Ba-PDMS3, which possess higher molar mass 11600 g/mol, was also proven by MALDI-TOF MS spectroscopy (**Figure S7**).

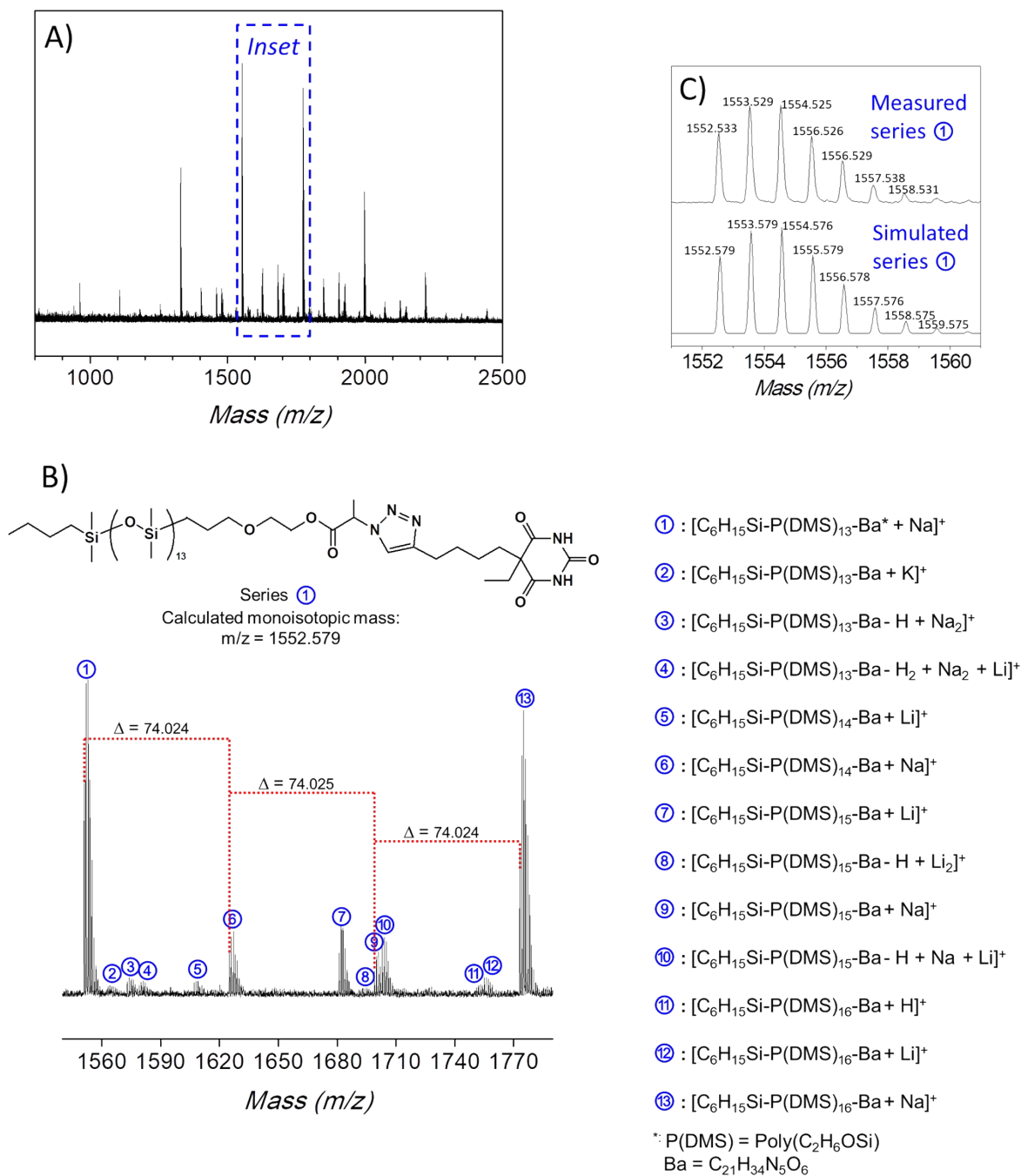


**Figure S5:** MALDI-TOF MS of Ba-PDMS1 (A) full spectrum, (B) expansion and (C) simulation of the isotope pattern.

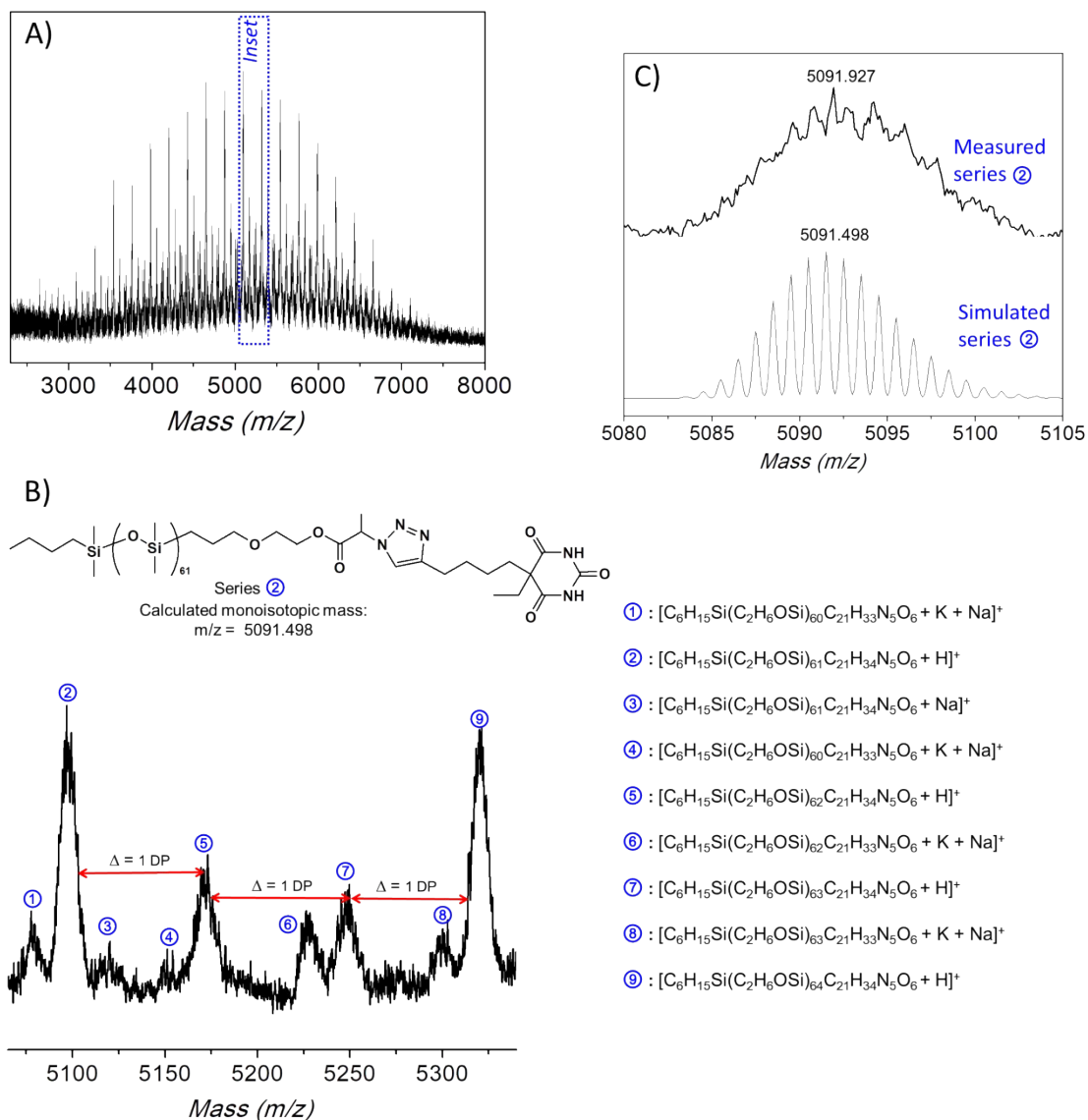


**Figure S6:** MALDI-TOF MS of Ba-PDMS2 (A) full spectrum, (B) expansion and (C) simulation of the isotope pattern.

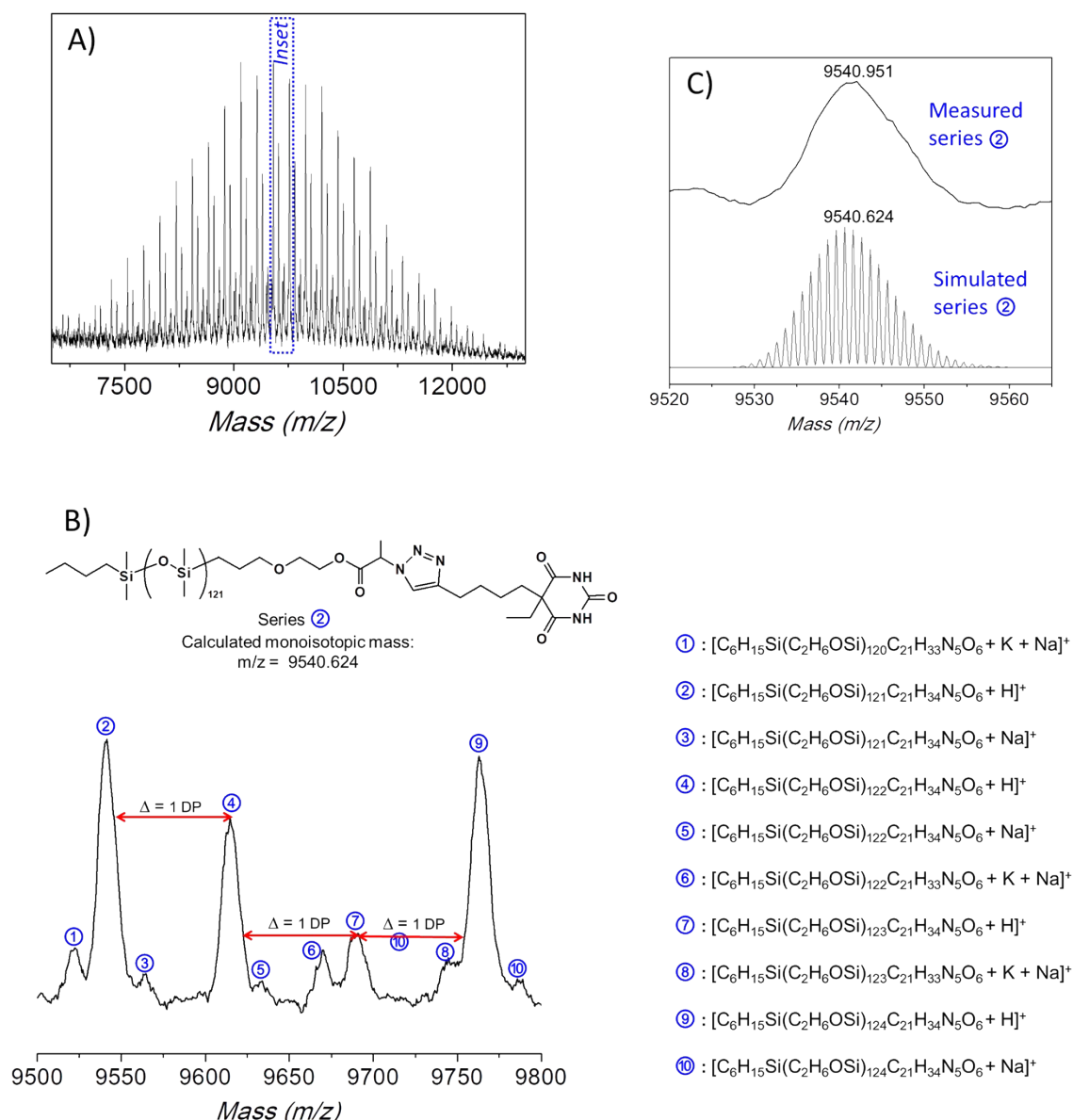


**Figure S7:** MALDI-TOF MS of Ba-PDMS3 (A) full spectrum, (B) expansion and (C) simulation of the isotope pattern.

## MALDI-TOF MS measurement of HW-PDMS1 and HW-PDMS3

The mass spectrum of HW-PDMS1 (**Figure S8**), acquired in the linear mode, disclosed the series  $\blacklozenge$ ,  $\blacklozenge$ ,  $\boxtimes$  and  $\wp$  separated by  $\sim 74.0$  g/mol mass units, i.e., a dimethylsiloxane repeat unit (**Figure S8B**). The main series  $\blacklozenge$  located at 1398.594 g/mol (**Figure S8C**) was corresponding to a HW functionalized species  $[\text{C}_6\text{H}_{15}\text{Si-P}(\text{DMS})_7\text{-HW} + \text{Na}]^+$ , i.e.,  $[\text{C}_6\text{H}_{15}\text{Si-}$

$P(C_2H_6OSi)_7-C_{37}H_{44}N_9O_8 + Na]^+$ , in good agreement with simulated pattern ( $m/z$  average = 1398.546 g/mol). As expected, the simulated and measured isotopic patterns of the other main and minor species were also well-matched (**Figure S8B**). In a similar manner, the structure of HW-PDMS3 (Mn = 11900 g/mol), was also evidenced by MALDI-TOF MS spectroscopy (**Figure S9**).

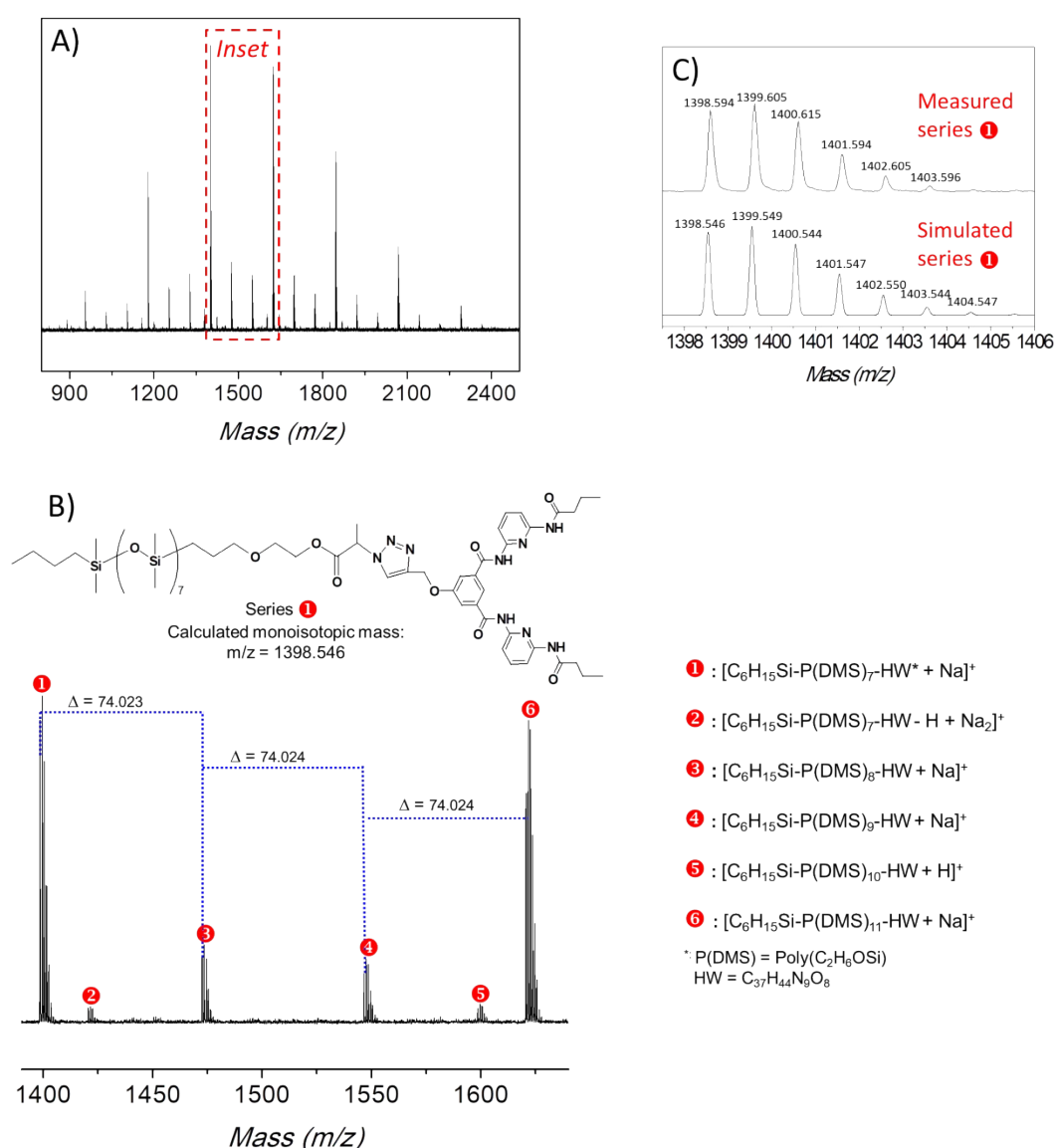


**Figure S8:** MALDI-TOF MS of HW-PDMS1 (A) full spectrum, (B) expansion and (C) simulation of the isotope pattern.

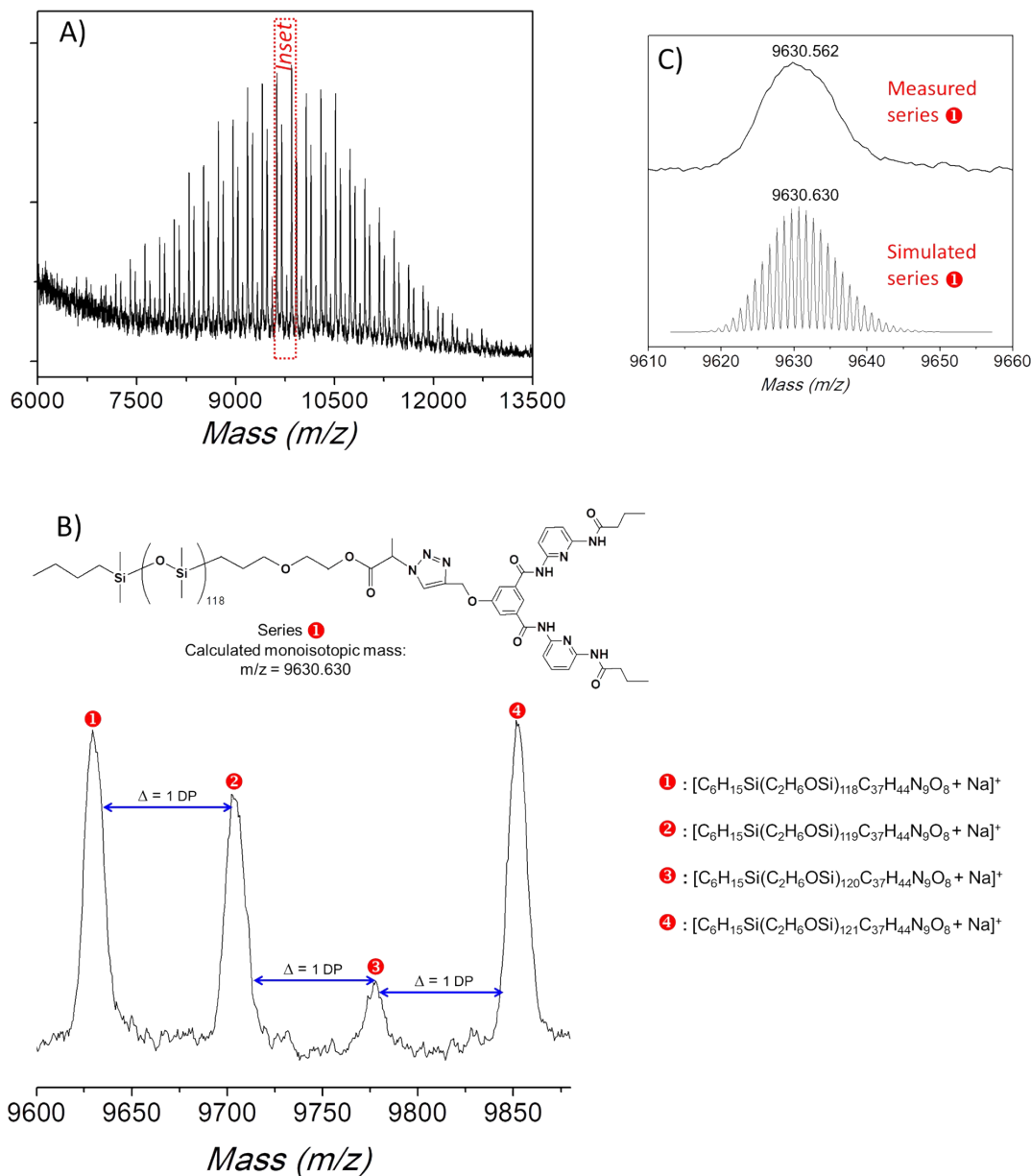


**Figure S9:** MALDI-TOF MS of HW-PDMS3 (A) full spectrum, (B) expansion and (C) simulation of the isotope pattern.

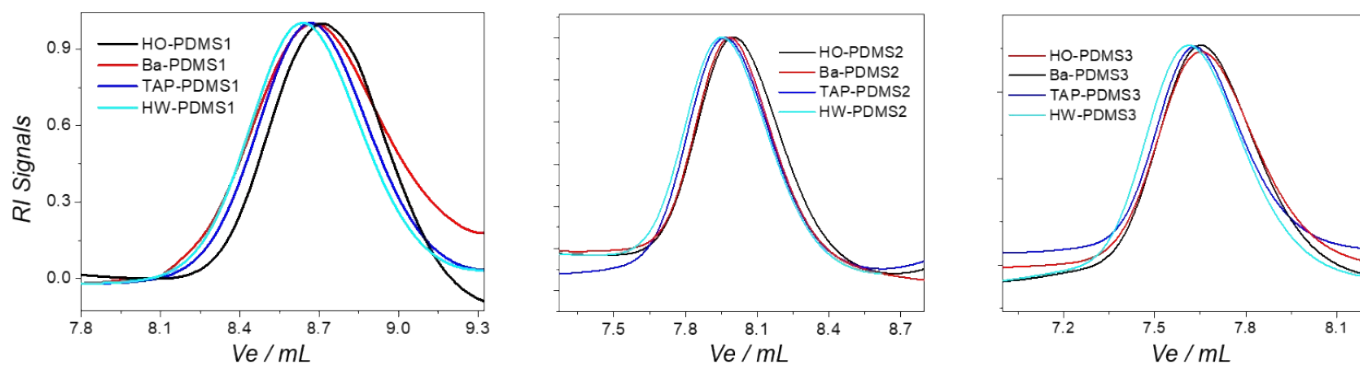


**Figure S10:** Evolution of the SEC traces of H-bonding PDMS.

## $^1\text{H}$ NMR spin-lattice relaxation time $T_1$ calculation.

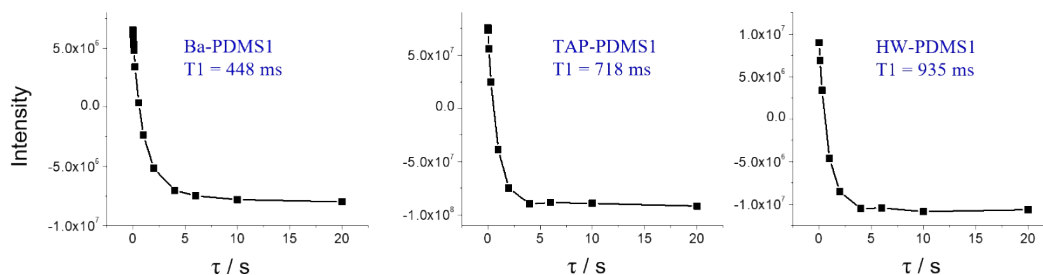


Figure S11:  $^1\text{H}$  NMR spin-lattice relaxation time  $T_1$  of Ba-PDMS1, TAP-PDMS1, and HW-PDMS1 at 27 °C.

## SAXS profile of HO-PDMS1.

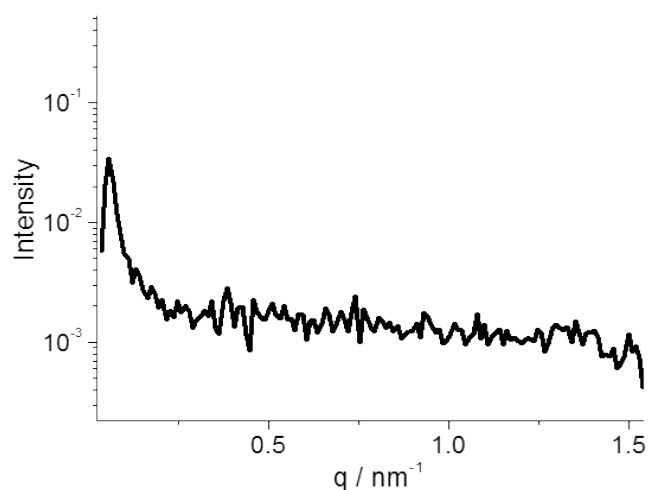


Figure S12: SAXS profile of HO-PDMS1 at 20 °C.

## Mathematical model chosen to determine $K_a$ between Ba-PDMS1 and TAP-PDMS1.

Data related to the concentration-dependence of the chemical shift of Ba  $\text{NH}$  proton for a mixture of a Ba-PDMS1 ( $[\text{Ba-P}] = 3 \times 10^{-3} \text{ mol} \cdot \text{L}^{-1}$ ) and TAP-PDMS1 were fitted according to the following equation to provide  $K_a$ :

$$\delta_{\text{mixt}} = \delta_{\text{Ba-P}} + \frac{(\delta_{\infty} - \delta_{\text{Ba-P}}) \left( ([\text{Ba-P}] + [\text{TAP-P}] + \frac{1}{K_a}) - \left( ([\text{Ba-P}] + [\text{TAP-P}] + \frac{1}{K_a})^2 - 4[\text{Ba-P}][\text{TAP-P}] \right)^{1/2} \right)}{2[\text{Ba-P}]}$$

where the experimental parameters are:  $[\text{Ba-P}]$  and  $[\text{TAP-P}]$ , the respective molar concentrations of Ba-PDMS1 and TAP-PDMS1;  $\delta_{\text{mixt}}$ , the measured NH chemical shift for Ba-P and TAP-P mixture;  $\delta_{\text{Ba-P}}$ , the measured NH chemical shift for TAP-P solution. The fitted parameters are:  $K_a$ , the association constant and  $\delta_{\infty}$ , the NH chemical shift of the fully associated system.

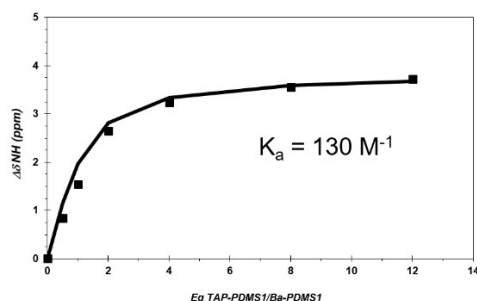


**Figure S13:** Concentration-dependence of the chemical shift of Ba NH proton for a mixture of Ba-PDMS1 ( $[\text{Ba}] = 3 \times 10^{-3} \text{ mol}\cdot\text{L}^{-1}$ ) and TAP-PDMS1 in  $\text{CDCl}_3$  at  $27^\circ\text{C}$  (filled symbols); fit corresponding to  $K_a = 130 \text{ M}^{-1}$  and  $\delta_{\infty} = 13 \text{ ppm}$  (curve).

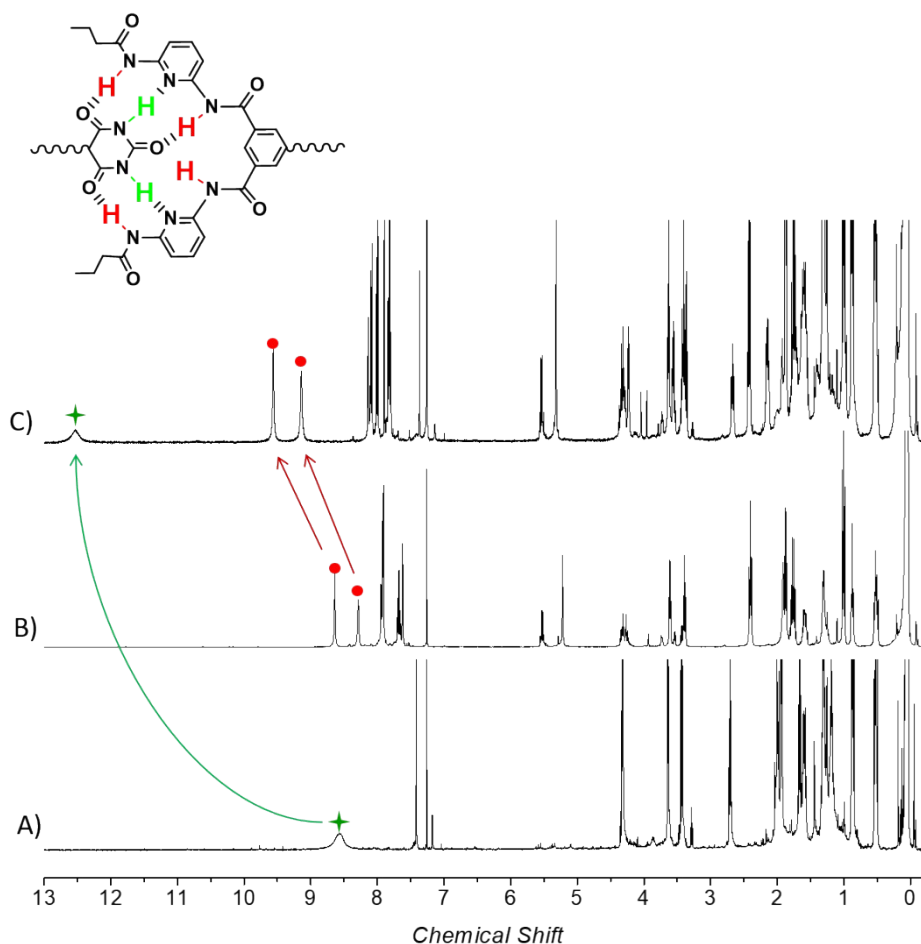


**Figure S14:** <sup>1</sup>H NMR spectra of Ba-PDMS1 (A), HW-PDMS1 (B), and a stoichiometric Ba-PDMS1/HW-PDMS1 mixture (C) at 27 °C in CDCl<sub>3</sub> ([Ba] = [HW] = 3 mM). Green cross: Ba NH protons, red spot: HW NH protons.

## Mathematical model chosen to determine $K_a$ between Ba-PDMS1 and HW-PDMS1.

Data related to the concentration-dependence of the chemical shift of Ba NH proton for a mixture of a Ba-PDMS1 ([Ba-P] =  $3 \times 10^{-3}$  mol·L<sup>-1</sup>) and HW-PDMS1 were fitted according to the following equation to provide  $K_a$ :

$$\delta_{\text{mixt}} = \delta_{\text{Ba-P}} + \frac{(\delta_{\infty} - \delta_{\text{Ba-P}}) \left( ([\text{Ba-P}] + [\text{HW-P}] + \frac{1}{K_a}) - \left( ([\text{Ba-P}] + [\text{HW-P}] + \frac{1}{K_a})^2 - 4[\text{Ba-P}][\text{HW-P}] \right)^{1/2} \right)}{2[\text{Ba-P}]}$$

where the experimental parameters are: [Ba-P] and [HW-P], the respective molar

concentrations of Ba-PDMS1 and HW-PDMS1;  $\delta_{\text{mixt}}$ , the measured NH chemical shift for Ba-P and HW-P mixture;  $\delta_{\text{Ba-P}}$ , the measured NH chemical shift for HW-P solution. The fitted parameters are:  $K_a$ , the association constant and  $\delta_{\infty}$ , the NH chemical shift of the fully associated system.

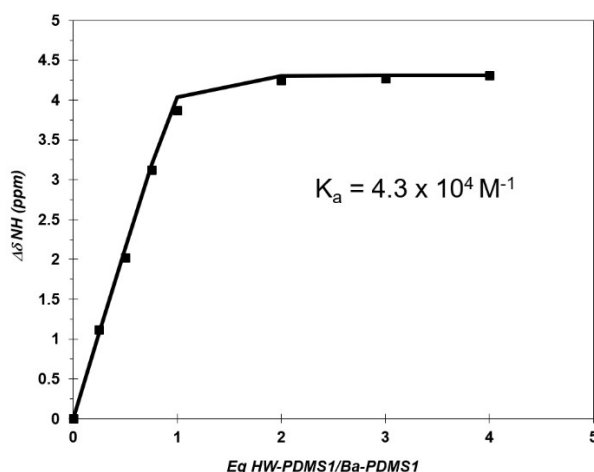


**Figure S15:** Concentration-dependence of the chemical shift of Ba NH proton for a mixture of Ba-PDMS1 ( $[\text{Ba}] = 3 \times 10^{-3} \text{ mol}\cdot\text{L}^{-1}$ ) and HW-PDMS1 in  $\text{CDCl}_3$  at  $27^\circ\text{C}$  (filled symbols); fit corresponding to  $K_a = 4.3 \times 10^4 \text{ M}^{-1}$  and  $\delta_{\infty} = 13 \text{ ppm}$  (curve).

## Viscosities of H-bonding PDMS.

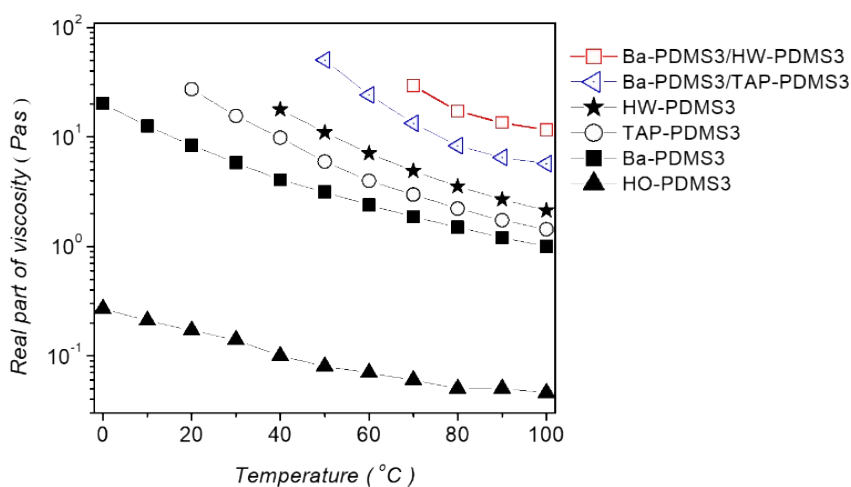


**Figure S16:** logarithmic plot of the real part of viscosity vs. temperature

## SAXS profiles of H-bonding PDMS.

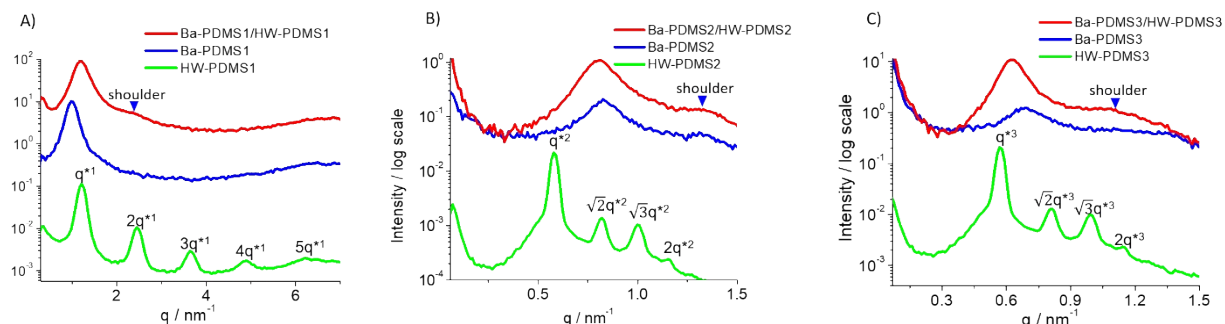


Figure S17: SAXS profiles of H-bonding PDMS at 20 °C.

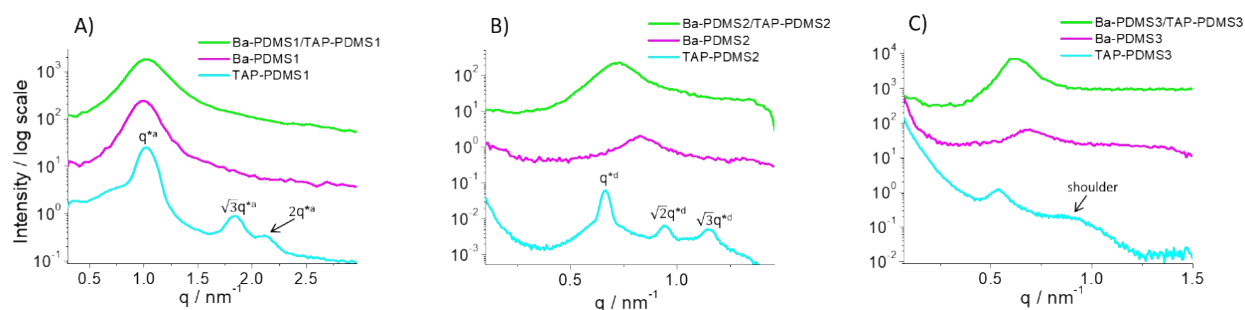


Figure S18: SAXS patterns of H-bonding PDMS at 20 °C.

## References

(1) Chen, S.; Yan, T.; Fischer, M.; Mordvinkin, A.; Saalwächter, K.; Thurn-Albrecht, T.; Binder, W. H.: Opposing Phase-Segregation and Hydrogen-Bonding Forces in Supramolecular Polymers. *Angew. Chem. Int. Ed.* **2017**, *56*, 13016-13020.

(2) Chen, S.; Wang, K.; Geng, Z.; Chen, Y.; Wang, H.; Zheng, X.; Zhu, J.: Construction and Morphology of Non-Covalently Double-Crosslinked Supramolecular Polymer Networks. *Polym. Chem.* **2019**, *10*, 4740-4745